Hindawi Publishing Corporation
Journal of Nanomaterials
Volume 2014, Article ID 503676, 7 pages
http://dx.doi.org/10.1155/2014/503676

Research Article

Synthesis and Characterization of Nanostructured Nickel Diselenide $NiSe_2$ from the Decomposition of Nickel Acetate, $(CH_3CO_2)_2Ni$

Ming Yin[1] and Stephen O'Brien[2]

[1] *GE Global Research, 1 Research Cir, Schenectady, NY 12309, USA*
[2] *Chemistry Department, The City College of New York, City University of New York, 160 Convent Avenue, New York, NY 10031, USA*

Correspondence should be addressed to Stephen O'Brien; sobrien@ccny.cuny.edu

Received 5 February 2014; Accepted 21 July 2014; Published 19 August 2014

Academic Editor: Jijun Qiu

Solution processed $NiSe_2$ nanorods were synthesized by a modified colloidal synthesis technique, by chemical reaction of TOPSe and nickel acetate at 150°C. The rods exist as an oleic acid ligand stabilized solution, with oleic acid acting as a capping group. Structural characterization by X-ray diffraction and transmission electron microscopy indicates that the particles are rod-like shaped crystals with a high and relatively constant aspect ratio (30 : 1). TEM shows that the width and the length of the nanorods are in the range 10–20 nm and 300–350 nm, respectively. XRD indicates that the nanorods are pure and well crystallized. The size of nanorods based on the Debye-Scherrer effect, was 150 nm, the average value of length and width. They display thermal stability over prolonged heating times (<100 hours) at 150°C, for which the average particle size is roughly constant. After about 100 hours of heating time there is an onset and growth of micron sized cubes and concurrent decomposition of $NiSe_2$ to Ni and NiSe at 150°C.

1. Introduction

Nanoparticles and nanowires, typically containing from hundreds to tens of thousands of atoms, high surface/volume ratios, size-dependent properties, and the possibility of arranging them in micro- (and nano)assemblies, have remained the focus of intensive research due to their numerous applications in diverse fields [1–3]. Nanoscale chalcogenides have attracted considerable attention due to their remarkable properties and application prospects [4]. Various interesting magnetic properties and crystallographic studies have been reported on transition metal dichalcogenides MX_2 (M = Fe, Co, and Ni; X = S, Se, and Te) with a pyrite structure, which is cubic, of space group T_h^6 (Pa_3). As typical representatives of the great number of transition metal chalcogenides, the selenides have been investigated extensively. MSe_2 are important direct band gap materials. Various methods have been developed to prepare transition metal selenides [5].

Nanoscale selenides are interesting to study the variation of a material's property with size and the ability to perform shape control. In recent years, the popularity of metal chalcogenide synthesis has soared due to (i) the discovery of graphene and an extension of pursing 2D atomic monolayer physics on van der Waals layered materials [6] and (ii) the observation of unique transport behavior in selenides such as Bi_2Se_3—materials identified as topological insulators [7]. $NiSe_2$ is one selenide that can be studied in this context for synthetic control over nanostructure [8–12]. Due to their unusual morphologies, the nickel selenides are also expected to find unique applications in energy research, such as electrochemistry, energy storage, and catalysis [13–15]. Elevating the temperature or pressure and extending the reaction period may create bigger single crystals, which provide an opportunity to investigate its fundamental properties [5, 16].

$NiSe_2$ has a pyrite structure (space group $T_h^6(Pa_3)$). Each metal atom is surrounded octahedrally by six metalloid atoms, and each metalloid atom is surrounded tetrahedrally by one metalloid atom and three metal atoms. $NiSe_2$ is a good electrical conductor. Its magnetic susceptibility is weakly paramagnetic (1×10^{-6} emu/g) and increases very

weakly with temperature and is therefore described as a Pauli paramagnetic metal. Now, $NiSe_2$ has been regarded as typical material for studies of the physical characteristics associated with a narrowband electron system [17–20].

Nickel diselenide was described for the first time by Fonzes-Diacon [20]. In 1900 a gray black mass of $NiSe_2$ was prepared by the action of hydrogen selenide on nickel(II) chloride at about 300°C. Nickel selenides have since been prepared by precipitation by the action of hydrogen selenide or potassium selenide on a nickel salt solution containing acetic acid and sodium acetate [21]. The structure of $NiSe_2$ was originally established by de Jong and Willem by X-ray diffraction studies on a sample prepared by heating a mixture of NiSe and selenium [22, 23].

Crystalline transition metal dichalcogenides can be synthesized by the direct stoichiometric combination of elements in evacuated silica tubes [24]. But due to the limit of slow diffusion, the complete reaction requires intermittent grinding and heating at high temperature from 500 to 1200°C. Parkin and coworkers improved direct elemental reactions by conducting them in liquid ammonia at room temperature, but the obtained product was a mixture of amorphous nickel selenide and crystalline element Ni [25, 26]. Novel organometallic precursors were also used to prepare transition metal diselenides: Steigerwald and coworkers reported that the reaction between bis(cyclooctadiene) nickel and tri(ethylphosphine selenide) at 270°C produced crystalline Ni_3Se_2 and elemental Ni that were difficult to be removed from the product [20, 27]. Wang et al. synthesized one-dimensional monoselenides by the reaction of metal chlorides, KBH_4, and selenium in ethylenediamine [28]. Zhang et al. synthesized $NiSe_2$ through a solvothermal reaction at low temperatures [29]. Han et al. reported the synthesis via the reaction of $NiC_2O_4{\cdot}2H_2O$ and elemental Se [30]. In that case, the molar ratios of reactants (Ni/Se) and temperature played important roles in determining the phase distribution. Adequate $NiC_2O_4{\cdot}2H_2O$ and higher temperature favor the formation of compounds with higher nickel contents. Excess selenium is essential to $NiSe_2$ and $Ni_{0.85}Se$ in pyridine, THF, and En. In water, sufficient nickel is necessary for $NiSe_2$. Zhang et al. reported a facile one pot synthesis to produce hollow spheres of PbSe and $NiSe_2$ [9]. Star [10, 31] and tubular [14] morphologies are also reported.

In this report we demonstrate that the reaction of nickel acetate stabilized with oleic acid and further reacted with trioctylphosphine selenide (TOPSe) which can be used to produce nanostructured $NiSe_2$.

2. Methods

2.1. Chemicals. The tri-*n*-octylphosphine (TOP), phenyl ether (DPF), oleic acid, selenium pellet, and nickel acetate ($(CH_3CO_2)_2Ni{\cdot}4H_2O$) were purchased from Sigma-Aldrich. Reagents were of analytical grade and were used without any further purification.

2.2. Stock Solution. Trioctylphosphine selenide (TOPSe) was prepared by adding appropriate mass of selenium pellet directly in sufficient stirring TOP in a dry box to produce 1.0 M stock solution of TOPSe. TOPSe was stored in the dry box.

2.3. Synthesis Procedure. 0.003 mol nickel acetate, 75 mL DPE, and 0.009 mol oleic acid (3 equivalent) were combined with nitrogen flow. The solution is dried and degassed in the reaction vessel by heating up to 150°C, flushing with 1 atm argon. All H_2O is removed during this process and $(CH_3CO_2)_2Ni$ results. The syringe containing 0.009 mol stock solution is quickly removed from the dry box and its contents delivered to the vigorously stirring reaction flask by a single injection through a rubber septum. The rapid introduction of the reagent mixture produces a gray solution. This is also accompanied by a sudden decrease in temperature. Heating is restored to 150°C. After maintaining the solution stirring at 150°C for 12–48 hr, the solution gradually turns to black.

Reaction was maintained at 150°C under 1 atm Ar. Aliquots of the reaction solution are removed at regular intervals. The reaction solution is cooled to 60°C. Addition of 10 mL methanol, 10 mL ethanol, and 2-3 mL butanol to the aliquot results in the reversible flocculation of the nanocrystallites. The flocculate is separated from the supernatant by centrifugation, which results in a clear solution containing methanol, ethanol, butanol, and byproducts of the reaction and black precipitates containing nanoparticles. The addition of 25 mL of hexane and 2-3 drops of oleic acid brings the particles back into solution. The particles are washed by methanol and ethanol two or three times until an optically clear solution is observed. After a final rinse of the flocculate with 50 mL methanol, the resulting particles are brought back into hexane for analysis and manipulation as suspension.

The reactions of $(CH_3CO_2)_2Co{\cdot}4H_2O$ and $(CH_3CO_2)_2Fe{\cdot}4H_2O$ under identical conditions did not produce a nanostructured material. To prepare FeSe as a comparison, $Fe(CO)_5$ was heated under the same solvent conditions to 230°C; then TOPSe was injected into the reaction vessel. FeSe nanoparticles quickly precipitated from the solution upon injection.

2.4. X-Ray Diffraction (XRD). X-ray powder diffraction patterns for different samples were determined on a Scintag X_2 X-ray diffractometer using nanochromated Cu-Kα1 radiation ($\lambda = 1.504$ A), employing a scanning rate of 0.02 deg·s^{-1} in the 2θ range from 20° to 60°. The samples for XRD measurements were prepared by dispersing particles in hexane and dropping onto the silicon wafer. Particles' sizes were estimated by the Debye-Scherrer formula according to XRD spectrum. Lattice parameter was also calculated.

2.5. Transmission Electron Microscopy (TEM). The morphology and particle size were studied by Philips EM430 transmission electron microscope using an accelerating voltage of 300 kv. Samples for TEM were deposited onto 400 mesh Cu grids coated with amorphous carbon films. To avoid the harmful effect of organic matter to the TEM, the grids were

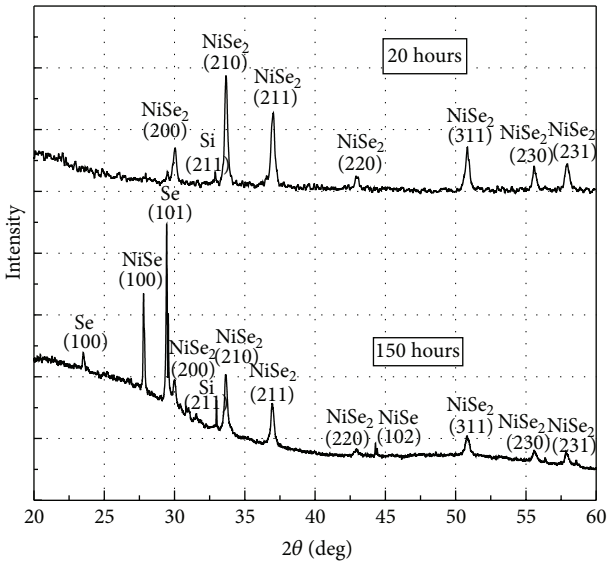

Figure 1: X-ray powder diffraction pattern of $NiSe_2$ particles. The reaction was maintained at 150°C and the product was analysed after 20 hours and 150 hours.

heated to 50°C in vacuum chamber for 10 hours and stored in a dry box.

3. Results and Discussion

$NiSe_2$ nanorods were synthesized by chemical reaction of TOPSe and nickel acetate at 150°C. The rods, with a high aspect ratio (30 : 1), exist as an oleic acid ligand stabilized solution in the presence of oleic acid as a capping group. Injection of TOPSe stock solution into the reaction flask yields a gray solution. The solution gradually turns to black indicating that large quantities of particles were produced after 20-hour reaction at 150°C. No obvious change was observed until some red precipitate was observed after 100 hours.

From the beginning of the reaction until 100 hours, all the samples share a similar X-ray diffraction pattern as shown in Figure 1, indicating a good crystallization and purity of the $NiSe_2$ particles. All peaks in the pattern can be indexed to cubic $NiSe_2$. No impurity phase was detected except the peak of Si (211), which was the background of the silicon wafer. The broadening of the peaks is due to Debye-Scherrer effect. The results of X-ray diffraction showed that, from the beginning of the reaction to 100 hours, pure and well-crystallized $NiSe_2$ crystals were precipitated. Calculated by Debye-Scherrer formula, the average particle size was 150 nm, which is in agreement with microscopy characterization. No obvious change was detected within 100 hours. However, as shown in Figure 1, the X-ray diffraction pattern of 150 hours consisted of peaks of NiSe and Se besides peaks of $NiSe_2$, which indicated that the $NiSe_2$ crystal was partially decomposed into Ni and NiSe. Also, the average particle size increased to 250–500 nm. With the longer reaction times an amorphous phase appeared. In this case, the X-ray substrate Si (211) peak, which is the background peak, is the only peak observed.

In the case of the $NiSe_2$ nanorods isolated prior to the 100-hour heating time, the crystal size, as shown in Figure 2, was about 150 nm during the reaction time from 40 hours to 100 hours. Because the particles were rod-like, with a large ratio of length to width, as shown in Figure 3(a), the size calculated from Debye-Scherrer equation should be the distribution average of the length and width. As measured by TEM pictures in Figure 3, the width and the length of crystal were 10–20 nm and 300–350 nm separately. Obvious particle growth was observed after 100 hours as the decomposition began. The particle size dramatically grew to 250–500 nm, with a shape change from rod-like to cubic, as shown is Figure 3. The lattice parameter calculated from X-ray pattern was 5.9634 Å, close to 5.9604 Å from the JCPDS card.

TEM images of the products under different reaction times are shown in Figure 3. Crystallized nanorods with a width of 10–20 nm and average lengths of 300–350 nm could be seen to evolve, especially in the timeframe from 40 hours to 100 hours. When the reaction time was prolonged to >100 hours, particles began to agglomerate into cubic particles. The growth of these cubic particles dramatically increased with increasing reaction time. When the reaction time was prolonged to 150 hours, the cubic particles were completely dominant with an average size of about 500 nm. With the even longer reaction times, the particles began to lose crystallinity confirmed by X-ray diffraction, and the shape of the particles also changed from cubic to amorphous.

4. Discussion of the Reaction Mechanism

The synthesis process over the prolonged reaction time of >100 hours can be divided into three stages: nucleation, growth, and ultimate amorphism. Following reaction, nuclei of $NiSe_2$ form, generating rod-like morphologies of 10–20 nm diameter. In the later stages (>100 hours, 150°C) a ripening and decomposition takes place in which cubic particles are observed to evolve, presumably based on the nanorods agglomerating and converting to crystalline cubic aggregates. These particles are bigger (250–500 nm) than the rod-like nucleus, as shown in Figure 3. In the final stage (>150 hours heating time), particles appeared to finally convert to NiSe and Se, with a loss of crystallinity observed by XRD.

In the experiment, the reactions took place as follows. In the beginning, TOPSe is prepared as in Scheme 1.

Second, the precursor of Ni source was prepared as in Scheme 2.

The equilibrium of the reaction is shifted by continuously removing gaseous acetic acid, $H_4C_2O_{2(g)}$, from the reaction; the final product was nickel oleic acid, which is also noted to be the actual precursor of the synthesis. The solution of nickel oleic acid is observed to be green due to the color of Ni^{2-}. As soon as the TOPSe was mixed with nickel oleic acid in DPE, a homogeneous nucleation of $NiSe_2$ occurred in the solution, which became gray/black (see Scheme 3).

$NiSe_2$ nanorods are precipitated from the solution. Oleic acid, $[CH_3(CH_2)_7CH{=}CH(CH_2)_7CO_2H]^-$, and TOP act as

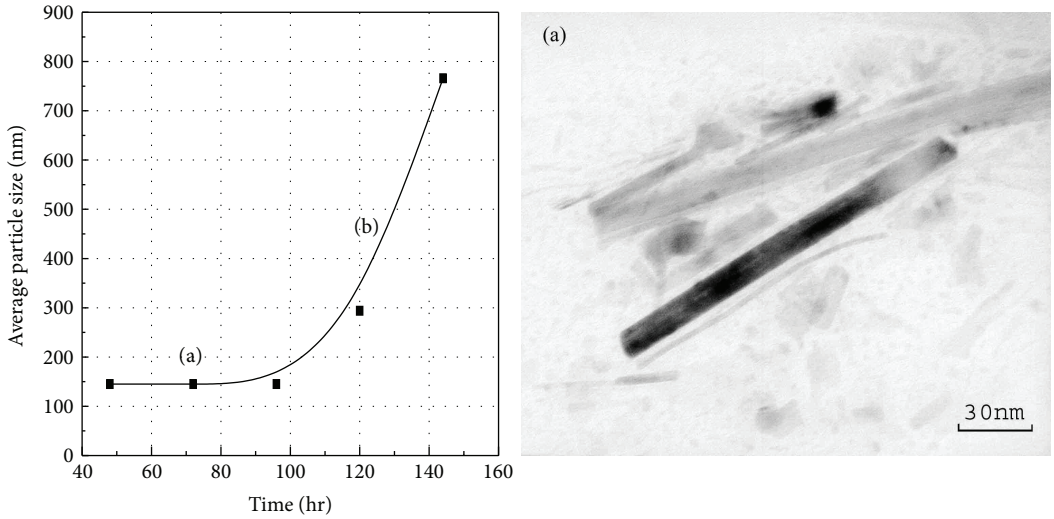

Figure 2: Particle growth with reaction time and TEM of section (a).

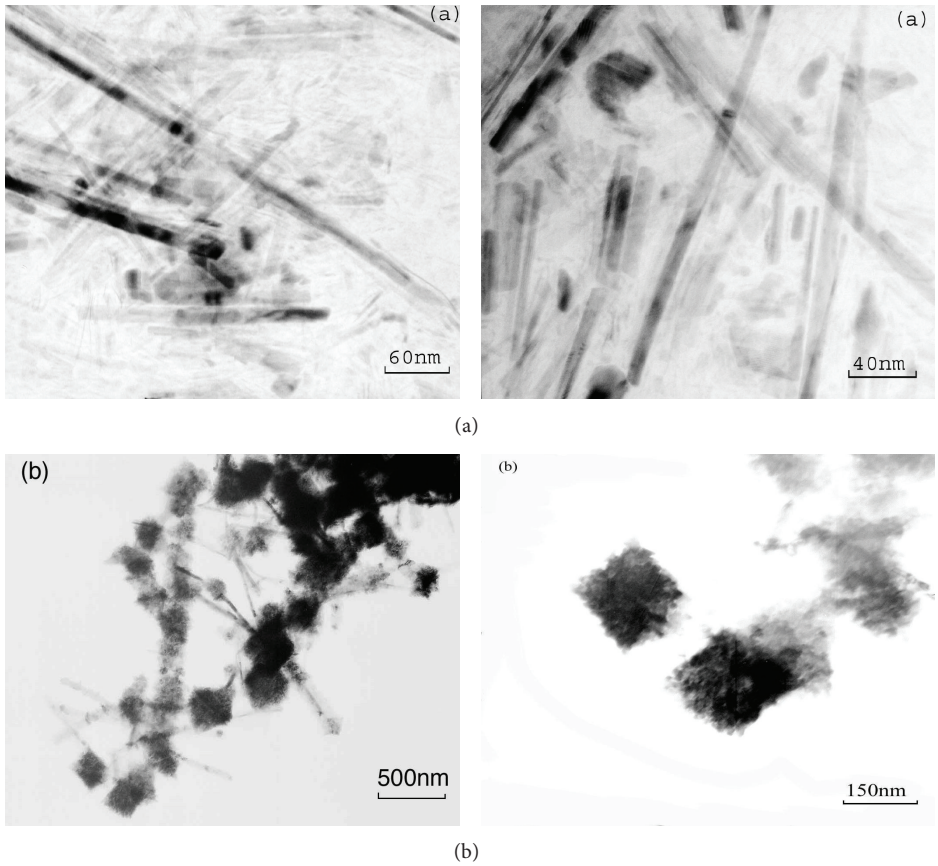

Figure 3: Sample TEM images of the products under different reaction times: (a) two images <100 hrs and (b) two images >150 hrs.

surfactants, coating the surface of $NiSe_2$ to prohibit the growth and agglomeration of the particles. It should be considered whether NiSe or $NiSe_2$ is the product, or a mixture results. If the valence state is considered, we deduce that $NiSe_2$ is the likely product. In this reaction, selenium loses two electrons, becoming Se^{2-}; the only donator could be Ni^{2+}, which becomes Ni^{4+}. So this reaction should proceed as $Ni^{2+} + Se^0 \rightarrow Ni^{4+} + Se^{2-}$. Second, $Ni^{4+} + 2Se^{2-} \rightarrow NiSe_2 \downarrow$. Whether it is possible to synthesize $NiSe_2$ or other transition metal dichalcogenides by this method is therefore determined by the ability of the electron donating power of metal cation. A similar reaction (metal oleate + TOPSe) was

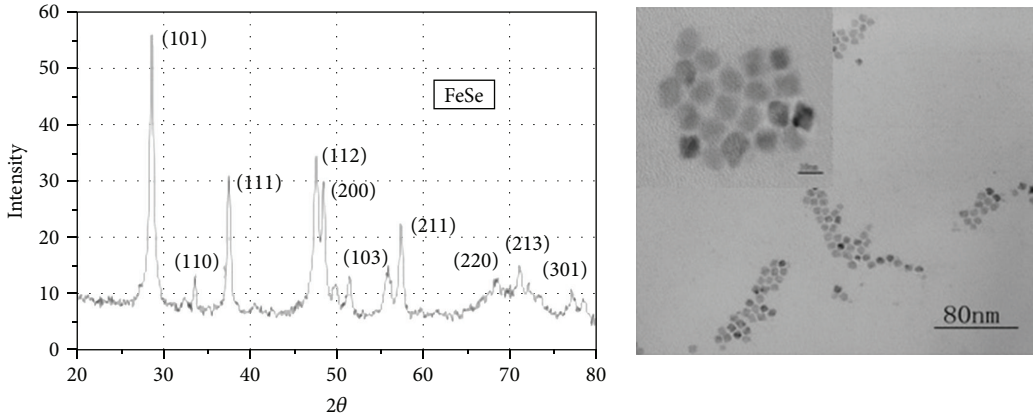

(a) (b)

Figure 4: FeSe produced from $Fe(CO)_5$. X-ray powder diffraction confirms the hexagonal NiAs-type structure, and morphology by TEM indicates roughly cubic nanoparticles of 10 nm size.

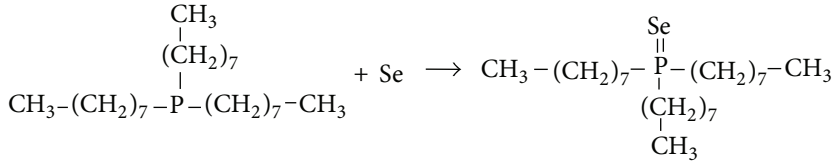

Scheme 1

performed using cobalt acetate to see whether or not $CoSe_2$ can be synthesized. Cobalt acetate was used in place of nickel acetate and the chemical reaction in the presence of TOPSe was conducted in an identical manner. Interestingly, in the case of cobalt acetate, no particle nucleation and growth was observed by this method. This is a striking contrast between the behaviors of Ni^{2+} and Co^{2+} under identical reaction environments. The explanation may possibly be because of the higher energy barrier from Co^{2+} to Co^{4+}. The standard reduction potential of Co^{2+} to Co^{4+} is +3.34, which is more than twice that of Ni^{2+} to Ni^{4+} (+1.59). In the case of cobalt, it is very difficult for Se^0 to capture two electrons from Co^{2+}. An explanation for the differing behavior of Ni and Co can be given, based on crystal/ligand field theory, in which the ligands are considered as point negative charges to be arranged in specific geometries (e.g., octahedral, tetrahedral). The splitting of the 3d orbitals within an octahedral crystal field expresses the splitting of energy levels in terms of the Δ_{oct} or 10Dq, the t_{2g} orbital symmetry set being relatively stabilized by $-0.4\Delta_{oct}$ or -4Dq while the e_g set is destabilized by $-0.6\Delta_{oct}$ or -6Dq. Since the compound forming is a selenide ion (weak field ligand) complex, growing into a crystal, it is reasonable to assume a small value of Δ_{oct} and generally high spin complexes. But in the case of $Ni^{4+}(3d^6)$ a $t_{2g}{}^6e_g{}^0$ configuration is likely favored—the t_{2g} is full and e_g is empty. So Ni^{2+} is more likely to donate two electrons, becoming Ni^{4+} and combining with Se^{2-}. However, for $Co^{2+}(3d^7)$, the d-orbital electrons are described as $t_{2g}{}^5e_g{}^0$ (Figure 4(b)) or $t_{2g}{}^6e_g{}^1$. However both are not particularly favorable since neither case yields a fully occupied subshell. The formation of $CoSe_2$ via oxidation of Co^{2+} to Co^{4+} can therefore be considered a less favorable route than that of nickel.

To test further whether a range of selenides can be formed by this process we applied the reaction chemistry to iron precursors in order to attempt the preparation of iron selenides. It was again found that the reaction of iron acetate, $(CH_3CO_2)_2Fe$, did not produce nucleation and growth, but that the decomposition of iron pentacarbonyl, $Fe(CO)_5$, under the same solvent conditions at higher temperature produced nanoparticles of FeSe (Figure 4). The particles are determined by TEM to be roughly cubic nanoparticles of 10 nm size, while X-ray powder diffraction confirms the hexagonal NiAs-type structure of FeSe. In this instance an oxidation of Fe^0 to Fe^{II} likely occurs in the event of reaction to produce FeSe.

For the synthesis of $NiSe_2$, interesting nucleation, growth, and precipitation occur alongside a change in phase and chemical exchange. The particles initially precipitate as $NiSe_2$ and nanorods form. In this stage, particles grow rapidly and the solution gradually became dark black. Decomposition of $NiSe_2$ particles appears to occur >100–125 hours reaction time at 150°C:

$$NiSe_2 \longrightarrow NiSe + Se \quad (1)$$

Besides the black precipitate, some red color was observed. The red color is believed to be from Se^{2-} for $[SeO_3]^{2-}$ or other polyselenide ions. It was concluded that $NiSe_2$ is kinetically stable, especially in the nanoscale, oleic

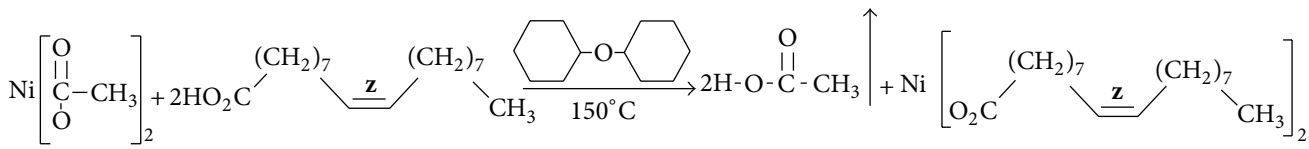

Scheme 2

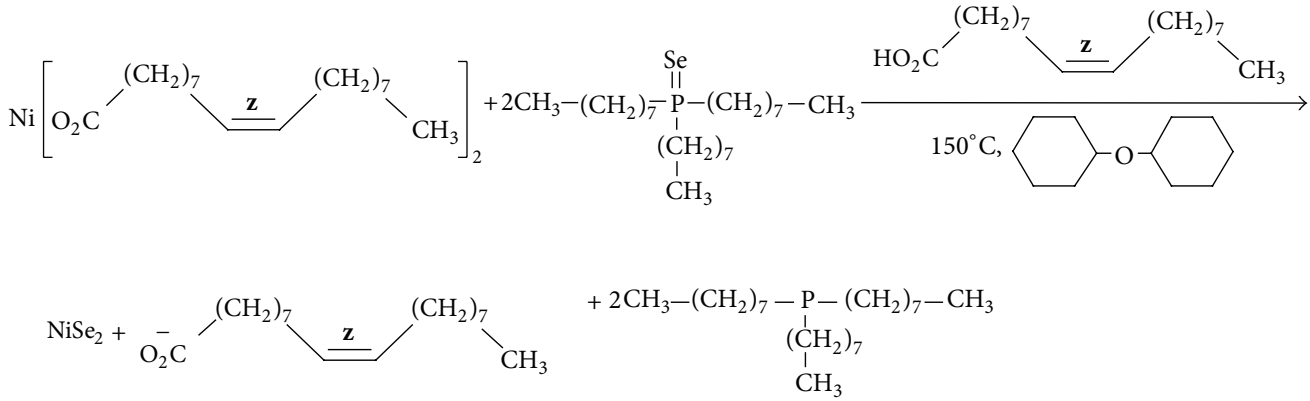

Scheme 3

acid stabilized form, but ultimately not thermodynamically stable at high temperature 150°C. Interestingly $NiSe_2$ is considered a more stable phase than NiSe, but in this reaction some $NiSe_2$ definitely decomposed to Ni and NiSe. With longer reaction times, these particles eventually became amorphous phase, with the color of the solution changing to black again.

5. Conclusion

In summary, $NiSe_2$ nanorods, with a large aspect ratio (30 : 1), have been synthesized by chemical reaction of TOPSe and nickel acetate, $Ni(CH_3CO_2)_2$, at 150°C. The rods exist as an oleic acid ligand stabilized solution in the presence of oleic acid as a capping group. After prolonged reaction times >100 hours at 150°C, the $NiSe_2$ became unstable and appeared to decompose to NiSe and Se. Reaction of $Fe(CH_3CO_2)_2$ $Co(CH_3CO_2)_2$ was also tested under identical reaction conditions. No particle formation was observed in the case of the acetates, whereas FeSe was formed with the use of zero valence $Fe(CO)_5$. These findings supported hypotheses that the reaction depends upon the ability of the metal cation to donate electrons to selenium in order to generate Se^{2-} and that the reduction potential of the ions will influence the outcome, whether MSe or MSe_2 is formed, or no reaction occurs.

Conflict of Interests

The authors declare that there is no conflict of interests regarding the publication of this paper.

Acknowledgments

Stephen O'Brien and Ming Yin thank Wolfgang Gaschler for useful discussions. Part of this work was conducted at Columbia University. Partial support is acknowledged from NSF MIRT no. 1122594. Support for this project was provided by a PSC-CUNY Award, jointly funded by The Professional Staff Congress and The City University of New York. Ming Yin is affiliated with GE Global Research, USA.

References

[1] F. J. Heiligtag and M. Niederberger, "The fascinating world of nanoparticle research," *Materials Today*, vol. 16, no. 7-8, pp. 262–271, 2013.

[2] M. Law, J. Goldberger, and P. Yang, "Semiconductor nanowires and nanotubes," *Annual Review of Materials Research*, vol. 34, pp. 83–122, 2004.

[3] J. K. Hyun, S. Zhang, and L. J. Lauhon, "Nanowire heterostructures," *Annual Review of Materials Research*, vol. 43, pp. 451–479, 2013.

[4] N. P. Dasgupta, J. Sun, and C. Liu, "25th anniversary article: semiconductor nanowires–synthesis, characterization, and applications," *Advanced Materials*, vol. 26, no. 14, pp. 2137–2184, 2014.

[5] T. A. Bither, R. J. Bouchard, W. H. Cloud, P. C. Donohue, and W. J. Siemons, "Transition metal pyrite dichalcogenides. High-pressure synthesis and correlation of properties," *Inorganic Chemistry*, vol. 7, no. 11, pp. 2208–2220, 1968.

[6] A. K. Geim and I. V. Grigorieva, "Van der Waals heterostructures," *Nature*, vol. 499, no. 7459, pp. 419–425, 2013.

[7] H. Peng, K. Lai, D. Kong et al., "Aharonov-Bohm interference in topological insulator nanoribbons," *Nature Materials*, vol. 9, no. 3, pp. 225–229, 2010.

[8] I. T. Sines and R. E. Schaak, "Phase-selective chemical extraction of selenium and sulfur from nanoscale metal chalcogenides: a general strategy for synthesis, purification, and phase targeting," *Journal of the American Chemical Society*, vol. 133, no. 5, pp. 1294–1297, 2011.

[9] G. Zhang, W. Wang, Q. Yu, and X. Li, "Facile one-pot synthesis of PbSe and NiSe2 hollow spheres: Kirkendall-effect-induced growth and related properties," *Chemistry of Materials*, vol. 21, no. 5, pp. 969–974, 2009.

[10] W. Du, X. Qian, X. Niu, and Q. Gong, "Symmetrical six-horn nickel diselenide nanostars growth from oriented attachment mechanism," *Crystal Growth and Design*, vol. 7, no. 12, pp. 2733–2737, 2007.

[11] S. A. Sunshine and J. A. Ibers, "Structure and physical properties of the new layered ternary chalcogenides Ta_2NiS_5 and Ta_2NiSe_5," *Inorganic Chemistry*, vol. 24, no. 22, pp. 3611–3614, 1985.

[12] T. K. Reynolds, J. G. Bales, and F. J. Disalvo, "Synthesis and properties of a new metal-Rich nickel antimonide telluride or selenide $Ni_{7-\delta}$ SBX_2 ($\delta \approx 1.3$; Se or Te)," *Chemistry of Materials*, vol. 14, pp. 4746–4751, 2002.

[13] A. Ennaoui and H. Tributsch, "Iron sulphide solar cells," *Solar Cells*, vol. 13, no. 2, pp. 197–200, 1984.

[14] H. Fan, M. Zhang, X. Zhang, and Y. Qian, "Hydrothermal growth of $NiSe_2$ tubular microcrystals assisted by PVA," *Journal of Crystal Growth*, vol. 311, no. 20, pp. 4530–4534, 2009.

[15] M. Xue and Z. Fu, "Lithium electrochemistry of NiSe2: a new kind of storage energy material," *Electrochemistry Communications*, vol. 8, no. 12, pp. 1855–1862, 2006.

[16] P. R. Bonneau, R. F. Jarvis Jr., and R. B. Kaner, "Rapid solid-state synthesis of materials from molybdenum disulphide to refractories," *Nature*, vol. 349, no. 6309, pp. 510–512, 1991.

[17] Y. Li, Y. Ding, Y. Qian, Y. Zhang, and L. Yang, "A solvothermal elemental reaction to produce nanocrystalline ZnSe," *Inorganic Chemistry*, vol. 37, pp. 2844–2845, 1998.

[18] T. Ohtani, M. Motoki, K. Koh, and K. Ohshima, "Synthesis of binary copper chalcogenides by mechanical alloying," *Materials Research Bulletin*, vol. 30, no. 12, pp. 1495–1504, 1995.

[19] G. Kräuter and W. S. Rees Jr., "Cadmium bis(alkylthiolate) complexes as precursors for cadmium sulfide: A mild route to hawleyite," *Journal of Materials Chemistry*, vol. 5, no. 8, pp. 1265–1267, 1995.

[20] J. G. Brennan, T. Siegrist, P. J. Carroll et al., "Bulk and nanostructure group II-VI compounds from molecular organometallic precursors," *Chemistry of Materials*, vol. 2, no. 4, pp. 403–409, 1990.

[21] M. Reeb, "L'Hydrogène Sélénié—Ses réaction sur les dissolutions métalliques," *Journal de Pharmacie et de Chimie*, vol. 9, pp. 173–176, 1869.

[22] W. F. De Jong and H. W. V. Z. Willems, "Structure of nickel diselenide," *Zeitschrift für Anorganische und Allgemeine Chemie*, vol. 170, article 241, 1928.

[23] F. Gronvold and E. Jacobsen, "X-ray and magnetic study of nickel selenides in the range NiSe to $NiSe_2$," *Acta Chemica Scandinavica*, vol. 10, pp. 1440–1454, 1956.

[24] T. Trindade, J. D. P. de Jesus, and P. O'Brien, "Preparation of zinc oxide and zinc sulfide powders by controlled precipitation from aqueous solution," *Journal of Materials Chemistry*, vol. 4, no. 10, pp. 1611–1617, 1994.

[25] G. Henshaw, I. P. Parkin, and G. Shaw, "Convenient, low-energy synthesis of metal sulfides and selenides; PbE, Ag2E, ZnE, CdE (E = S, Se)," *Chemical Communications*, vol. 2, no. 10, pp. 1095–1096, 1996.

[26] G. Henshaw, I. P. Parkin, and G. A. Shaw, "Convenient, room-temperature liquid ammonia routes to metal chalcogenides," *Journal of the Chemical Society: Dalton Transactions*, no. 2, pp. 231–236, 1997.

[27] J. G. Brennan, T. Siegrist, Y.-. Kwon, S. M. Stuczynski, and M. L. Steigerwald, "Ni23Se12(PEt3)13. an intramolecular intergrowth of NiSe and Ni," *Journal of the American Chemical Society*, vol. 114, no. 26, pp. 10334–10338, 1992.

[28] W. Wang, Y. Geng, P. Yan, F. Liu, Y. Xie, and Y. Qian, "A novel mild route to nanocrystalline selenides at room temperature," *Journal of the American Chemical Society*, vol. 121, no. 16, pp. 4062–4063, 1999.

[29] W. Zhang, Z. Hui, Y. Cheng, L. Zhang, Y. Xie, and Y. Qian, "Hydrothermal method for low-temperature growth of nanocrystalline pyrite nickel diselenide," *Journal of Crystal Growth*, vol. 209, no. 1, pp. 213–216, 2000.

[30] Z. Han, S. Yu, Y. Li et al., "Convenient solvothermal synthesis and phase control of nickel selenides with different morphologies," *Chemistry of Materials*, vol. 11, no. 9, pp. 2302–2304, 1999.

[31] J. Li, Z. Jin, T. Liu, J. Wang, X. Zheng, and J. Lai, "Chemical synthesis of MSe_2 (M = Ni, Fe) particles by triethylene glycol solution process," *CrystEngComm*, vol. 16, pp. 6819–6822, 2014.